

SR1—a small RNA with two remarkably conserved functions

Matthias Gimpel¹, Heike Preis¹, Emanuel Barth¹, Lydia Gramzow² and Sabine Brantl^{1,*}

¹AG Bakteriengenetik, Lehrstuhl für Mikrobiologie und Mikrobengenetik and ²Lehrstuhl für Genetik, Biologisch-Pharmazeutische Fakultät, Friedrich-Schiller-Universität Jena, Philosophenweg 12, Jena D-07743, Germany

Received January 23, 2012; Revised September 3, 2012; Accepted September 4, 2012

ABSTRACT

SR1 is a dual-function sRNA that acts as a base-pairing regulatory RNA on the *ahrC* mRNA and as a peptide-encoding mRNA on the *gapA* operon. The SR1-encoded peptide SR1P binds GapA thereby stabilizing *gapA* mRNA. Under glycolytic conditions, SR1 transcription is repressed by CcpN and CcpA. A computer-based search identified 23 SR1 homologues in *Bacillus*, *Geobacillus*, *Anoxybacillus* and *Brevibacillus* species. All homologues share a high structural identity with *Bacillus subtilis* SR1, and the encoded SR1P peptides are highly similar. In the *Bacillus cereus* group, the *sr1p* region is present in triplicate or duplicate resulting in longer SR1 species. In all cases, *sr1* expression is under control of CcpN, and transcriptional *lacZ* fusions of nine examined SR1 homologues were sensitive to glucose. Two homologues showed an additional glucose-independent repression by CcpN and an unknown factor. A total of 10 out of 11 tested SR1P homologues complemented a *B. subtilis* Δ *sr1* strain in their ability to stabilize *gapA* mRNA, but only five of them bound GapA tightly. *In vitro* binding assays with six SR1/*ahrC* pairs suggest that—despite divergent primary sequences—the base-pairing function is also preserved. In summary, SR1 is an sRNA with two functions that have been conserved over \approx 1 billion years.

INTRODUCTION

Small RNAs (sRNAs) are the largest class of post-transcriptional regulators in bacteria known to date (for reviews see (1, 2)). About 140 sRNAs are known in *Escherichia coli* and *Salmonella*. However, only about 25

of them have been assigned a biological function, indicating that defining their functions continues to be a challenging issue. In the last 3 years, systematic searches have been performed for several Gram-positive species (e.g. *Bacillus subtilis* (3, 4), *Listeria monocytogenes* (5), *Staphylococcus aureus*, (6, 7)) indicating that a plethora of sRNAs exists also in such genomes. sRNAs can be divided into two major groups: the first group regulate gene expression by a base-pairing mechanism with target mRNA, whereas the second group act by binding of small proteins. The major regulatory mechanisms applied by both cis- and trans-encoded base-pairing sRNAs include inhibition or activation of translation and promotion of RNA degradation or RNA stability. Additionally, inhibition of primer maturation, transcriptional attenuation and transcriptional interference have been found for some cis-encoded sRNAs (rev. in (8)). Interestingly, a few trans-encoded sRNAs have dual functions: they act both as base-pairing sRNAs and as peptide-encoding mRNAs. The first reported example was *S. aureus* RNAIII, which encodes δ -hemolysin (26 aa) and activates translation of *hla* mRNA (9) and, additionally, represses translation of *spa*, *rot*, *sa1000/2353*, *coa* (10). Later, the streptolysin SLS-ORF of *Streptococcus* Pel RNA (11) and the 43-codon-SgrT ORF on *E. coli* SgrS (12) were identified. SgrS and SgrT downregulate PtsG glucose transporter activity and have a physiologically redundant, but mechanistically distinct function in inhibition (12). In contrast, for the *hyp7*-ORF on *Clostridium perfringens* VR (13), the 37-codon PhrS-ORF of *Pseudomonas aeruginosa* (14), the 32-codon RivX-ORF (15) and the R5S0019-ORF of *Rhodobacter sphaeroides* (16) no functions have been elucidated so far.

The 205 nt RNA SR1 from the *B. subtilis* genome was found in our group by a combination of computer predictions and northern blotting (NB) (17). Previously, we have shown that SR1 acts by base pairing with its primary target, *ahrC* mRNA, the transcriptional activator of the *rocABC* and *rocDEF* arginine catabolic operons (18).

*To whom correspondence should be addressed. Tel: +49 3641 949570; Email: sabine.brantl@rz.uni-jena.de

The authors wish it to be known that, in their opinion, the first two authors should be regarded as joint First Authors.

SR1 inhibits translation initiation of *ahrC* mRNA by a novel mechanism: induction of structural changes downstream from the ribosome-binding site (19). SR1 is expressed under gluconeogenic and repressed under glycolytic conditions by CcpN, and, to a minor extent, CcpA (17). Thereby, CcpN requires ATP and a slightly acidic pH (20) to prevent promoter escape *via* direct contacts with the α -subunit of the *B. subtilis* RNA polymerase (21). Recently, we found that the 39-codon ORF on SR1 is translated into a peptide, designated SR1P. We demonstrated that SR1P binds GapA, thereby stabilizing the *gapA* operon mRNA by a hitherto unknown mechanism (22). SR1 is the first dual-function sRNA in *B. subtilis*.

Here, we provide a combination of a computer-based analysis of 23 SR1 and SR1P homologues from different Bacillales species and the *in vivo* and *in vitro* characterization of SR1 and SR1P homologues. We chose representatives of the two important *Bacillus* groups, the *B. subtilis* and the *B. cereus* group as well as from ungrouped Bacilli like *B. megaterium*, *B. halodurans* and *Geobacillus kaustophilus* for *in vivo* studies. All tested homologues were repressed by CcpN under glycolytic and expressed under gluconeogenic conditions. The two CcpN binding sites (BSs) were located at the same positions as in the *B. subtilis sr1* gene. Whereas 10 of 11 SR1P homologues were functional in NB to stabilize *B. subtilis gapA* mRNA, only 5 SR1P homologues were able to bind *B. subtilis* GapA tightly indicating that their interaction with GapA is stronger than that of the other homologues. The computer-based analysis of the regions required for base pairing with the *ahrC* mRNA homologues predicted between 7 and 11 complementary regions. *In vitro* binding assays with six SR1/*ahrC* pairs revealed that the base-pairing function of SR1 is preserved. Eight SR1 homologues could be detected in their native hosts, but expression of *B. pumilus* SR1 seems to be repressed. In summary, we found that both SR1 functions—the base-pairing and the mRNA function—have been conserved during 0.9–1.3 billion years of evolution.

MATERIALS AND METHODS

Identification of SR1P homologues

The amino acid (aa) sequence of *B. subtilis* SR1P was used as a query in a BlastP search against the non-redundant protein sequence database at NCBI. Using the SR1P homologues found in the first search, the consensus sequence MGTIV CQXC(EN) XTIXH FEDEK (VTS)T(VT) LY G (KT) CXX XCXCX XXXXX XXX was derived. Using this consensus sequence as a query in an additional BlastP search against the same database resulted in more homologous proteins. Results from all searches were corrected with regard to redundancy, resulting in a list of 23 SR1P homologues. The aa sequences of the 23 SR1P homologues were aligned using ClustalW (Blosum protein weight matrix, 23).

Identification of SR1 homologues

The *sr1* nucleotide sequence of *B. subtilis* was used as a query in a BlastN search against the Nucleotide collection

database at NCBI. Furthermore, the sequences adjacent to all *sr1p*-encoding regions were analysed. Analyses of the loci of all obtained nucleotide sequences indicated the location of the *sr1* homologues between the *pdhD* and the *speA/cad* genes. Investigation of the predicted *sr1* locus in other *Bacillus* and *Geobacillus* species yielded a few more homologous sequences.

Phylogeny reconstruction

SR1 sequences from species of the *Bacillus cereus* group were split in two and three parts, respectively, each beginning at the characteristic RNA stem-loop structure and ending at the stop codon of the putatively encoded peptide. The resulting sequences and the SR1 sequence of *Geob. kaustophilus*, which was later used as a representative of the outgroup in the phylogeny, were aligned using MAFFT (24). A MODELTEST (25) was performed to determine the best-fitting model for the alignment. Using this model, a phylogeny was reconstructed using MrBayes (26), where 3 000 000 generations were generated, the burn in was set to 750 000 and a majority rule consensus tree including all compatible groups was constructed. Using the same methods, a second phylogeny containing the consensus sequence of the three copies of the *Bacillus cereus* group and SR1 units of other *Bacillus* species having only one copy of the dual-function RNA was determined.

Identification of base-pairing determinants in SR1 homologues

The aa sequence of *B. subtilis ahrC* was used as a query to identify *ahrC* homologues with BlastP in each species containing an *sr1* homologue. IRNA, a local RNA–RNA interaction prediction tool (E. Barth, unpublished) was used to create interaction profiles between different regions of SR1 and *ahrC* mRNA based on the known interaction regions of *B. subtilis* SR1 and *ahrC* mRNA (18,19). IRNA determined optimal interaction profiles by optimizing a weighted base-pairing score as well as the total number of interactions.

Identification of CcpN and CcpA BSs in the promoter region of *sr1* homologues

A simple string-matching algorithm was applied to identify BS of CcpN and CcpA in *sr1* homologues. The consensus sequences used were 5' WTGNAANCG NWNNCW for the *cre* site (CcpA BS) and 5' TRTGHYATAYW (27) for the CcpN BS. The search was limited to the range between the SD sequence and 400 nt upstream of the *sr1* transcriptional start site. Thereby, only hits with a maximum of two mismatches compared to the consensus sequences were allowed.

Strains and growth conditions

Bacillus subtilis strain DB104 (28), *B. amyloliquefaciens* FZB42, *B. licheniformis* ATCC14580, *B. pumilus* DSM27, *B. thuringiensis* DSM350, *B. megaterium* DSM319, *B. halodurans* DSM497 and *Geob. kaustophilus* DSM7263 were used. All strains are considered to be

wild-type strains. They were grown at 37°C except *Geob. kaustophilus* that was grown at 54°C. TY medium was used as complex medium (18). For *B. halodurans*, TY was supplemented with 100 mM Na-sesquicarbonate pH 9.7.

Preparation of total RNA, RNA gel electrophoresis and NB

Preparation of total RNA, RNA gel electrophoresis on 6% denaturing polyacrylamide gels or 1.5% agarose gels and NB were carried out as described previously (18). For the detection of SR1 from *B. amyloliquefaciens* and *B. licheniformis*, the hybridization probe for *B. subtilis* SR1 was used. In contrast, separate probes had to be generated for the detection of the other SR1 homologues. The same holds true for the oligonucleotide probes against 5S rRNA used for reprobing (Supplementary Table S1).

Isolation of chromosomal DNA from different *Bacillus* species

Chromosomal DNA from all strains was isolated as described previously for *B. subtilis* (17).

Construction of plasmids for tet-inducible overexpression of *sr1* homologues and mutants

A polymerase chain reaction (PCR) on chromosomal DNA of the different *Bacillus* species was performed with primers designed on the basis of the *sr1* sequence retrieved from the NCBI database (primers are listed in Supplementary Table S1). The resulting fragments were subjected to a second PCR with primer SB1402 to add the Strep-tag sequence and the SR1 terminator from *B. subtilis* at the 3' terminus, digested with HindIII and inserted into the pWSR1-HindIII vector. The sequence was confirmed. In the case of pWSR1/M60 (plasmids are listed in Supplementary Table S2) designed to analyse the effect of the native triplicate *sr1* locus of *B. thuringiensis* in *B. subtilis*, only a single PCR reaction with the corresponding primer pair was performed, the resulting fragment digested with PstI and Acc65I cloned into the pWSR1 vector cleaved with the same enzymes. For the construction of pWSR1 derivatives comprising mutated *B. subtilis sr1* genes, two single PCRs with mutant primer 1 and SB317 and mutant primer 2 and SB348 were performed, followed by a second PCR with primers SB317 and SB348. The final PCR fragment was digested with HindIII and inserted into the pWSR1-HindIII vector.

Construction of plasmids for transcriptional *lacZ* fusions and determination of β -galactosidase activity

The upstream regions of different *sr1* species were amplified by PCR on chromosomal DNA of the corresponding *Bacillus* species as above using the primer pairs listed in Supplementary Table S1. The resulting fragments were digested with EcoRI and BamHI and cloned into pACC1 vector (22) cleaved with the same enzymes. In the wild-type cases, fragments were obtained that contained 87 bp upstream of the -35 box of *p_{sr1}*, the

promoter and 10 nt downstream from the putative transcription start site. Additionally, plasmids with sequences from the *sr1* homologues of *B. subtilis*, *B. megaterium* and *B. halodurans* were constructed that contained either only the promoter regions without regions upstream of the -35 boxes (pACS63, pACS65 and pACS67, respectively) or the promoter regions including only both CcpN BSs (pACS62, pACS64 and pACS66, respectively). The resulting plasmids were linearized with ScaI and inserted into the *amyE* locus of the *B. subtilis* DB104 chromosome by double crossing over. The resulting integrant strains were used for the determination of β -galactosidase activities as described previously (29).

Co-elution experiments with SR1P homologues and *B. subtilis* GapA

Co-elution experiments with Strep-tagged SR1P homologues and western blotting were performed as described recently (22).

Analysis of RNA-RNA complex formation

Both *ahrC* mRNA and SR1 were synthesized *in vitro* from PCR-generated template fragments with primer pairs indicated in Supplementary Table S1. SR1/*ahrC* complex formation studies were performed as described previously including tRNA as unspecific competitor (18).

Primer extension and 3' RACE

Primer extension was performed as described previously (17). 3' RACE was also performed as described (17), but with the following modifications: Total RNA from *B. thuringiensis* was ligated to intrinsic 16S rRNA instead to an artificial RNA adapter. Two subsequent PCR amplification steps were used, the first with outer primers SB1900/SB1894, and the second, nested PCR with inner primers SB1901/SB1897.

RESULTS AND DISCUSSION

Identification and gene synteny of 23 homologues of SR1

As we could show recently, the 39 aa ORF on *B. subtilis* SR1 is translated into a small peptide, SR1P, which was also found in some other Bacilli (22). To ascertain, whether SR1P is confined to *Bacillus* and *Geobacillus* species or is also present in other bacteria, a systematic search among all annotated bacterial genomes was undertaken as described in Materials and Methods section. This search identified 23 SR1 homologues, among them 18 *Bacillus* species, three *Geobacillus* species and, additionally, *Anoxybacillus flavithermus* WK1 and *Brevibacillus brevis* NBRC100599. A gene encoding SR1P was not found in *B. selenitireducens* and *B. cellulosityticus*. No *sr1* homologues were discovered in Gram-negative or in other Gram-positive bacteria. The gene synteny of 21 homologues is presented in Supplementary Figure S1. In all but one case, the *sr1* genes are located between *pdhD* and *speA/cad* genes, but the number of genes between *pdhD* and *sr1* on the one hand and *sr1* and *speA/cad* on the other hand, differed.

Whereas in all cases except for the *B. cereus* group and *Brev. brevis*, *speA* encoding arginine decarboxylase or *cad* encoding lysine decarboxylase was located immediately downstream from *sr1*, in the *B. cereus* group, *tgl* encoding transglutaminase was located between *sr1* and *speA/cad*, and in *B. mycooides*, *tgl* and gene 35 850 were located between *sr1* and *speA*. In *Brev. brevis*, five genes interrupted the *sr1* and the *speA* gene. The region upstream of *sr1* diverged much more with 6 and 10 genes located between *pdhD* and *sr1* in *B. pseudofirmus* and *B. halodurans*, respectively, whereas in *B. subtilis* and *B. pumilus*, *pdhD* and *sr1* were only separated by the *slp* gene. An alignment of all 23 SR1 sequences is presented in Supplementary Figure S2.

Based on the conserved location of the *sr1* gene in the Bacillales, we searched upstream of the *cad/speA* genes in other Gram-positive bacteria for putative *sr1* homologues, however, with no result.

Phylogeny

As summarized in Supplementary Table S3, most of the *sr1* genes contain a bidirectional terminator shared with the downstream gene transcribed into the opposite direction. In contrast, the *sr1* homologues of *B. clausii*, *B. coagulans*, *Anoxybacillus*, *Brevibacillus* and the three *Geobacillus* species carry unidirectional transcription terminators at their 3' ends. Their downstream genes have their own terminators. All SR1 homologues, except those from the *B. cereus* group, were predicted to be about 200–230 nt long. The latter group has *sr1* genes with triplicate or duplicate *sr1p* sequences, resulting in ≈ 600 nt or ≈ 400 nt long SR1 species comprising 3 subunits each coding for a peptide (SR1 I, SR1 II and SR1 III), respectively. The SR1 homologues from the *B. subtilis* group and *B. pumilus* are closely related and form a clade (Supplementary Figure S3). In this clade, the identity on nucleotide level for the *sr1p* coding region is between 83% and 92%. The *B. clausii* and *B. pseudofirmus* SR1 species are at the basal positions in the phylogeny and form a grade, but even their *sr1p* coding regions are between 81% and 84% identical with that of *B. subtilis*. Not surprisingly, the SR1 homologues from the three *Geobacillus* species cluster together and are more related to the *B. cereus* group than the SR1 species from the other Bacilli. *B. megaterium*, *B. coahuilensis*, *B. coagulans* and *Anoxybacillus* form a clade.

The presence of triplicate or duplicate *sr1p* genes prompted us to elucidate the order of duplications that gave rise to the additional *sr1p* copies. Therefore, we conducted an additional analysis. The resulting phylogeny reveals that there are three clades containing the copies I, II and III, respectively, distinguished (Figure 1). All three clades are comprised of copies from all species of the *B. cereus* group with the exception of clade III where *B. cytotoxicus* is missing as this species has only two SR1P copies. According to our phylogeny, copy III is the basal *sr1* copy. This copy was duplicated in a common *B. cereus* group ancestor resulting in SR1 III and a SR1 I/II precursor. This precursor was duplicated once more resulting in SR1 I and SR1 II each of them encoding a peptide.

The fact that the corresponding copies of the different species are more closely related to each other than the different copies of the same *Bacillus* species suggests that the most recent common ancestor of the *B. cereus* group Bacilli had already three SR1P copies. All three copies were retained during speciation events giving rise to the different *B. cereus* group members apart from *B. cytotoxicus* that lost the basal SR1P III copy.

Since SR1 is regulated by CcpN, but the *ccpN* gene is not located in the vicinity of the *sr1* gene, it was not possible to use the *ccpN* gene for a bioinformatics search for *sr1* homologues as it was done by Horler and Vanderpool for SgrS/SgrR (30). However, we currently develop a programme that allows predicting small peptides in different bacteria. This programme will be applied to search for functional homologues (which might differ in primary nt and aa sequence) for SR1 and SR1P downstream from CcpN BSs.

Comparison of the corresponding *sr1* promoter regions and the CcpN and CcpA BSs

The *B. subtilis* *sr1* gene is transcribed from a perfect consensus promoter with the –35 box TTGACA and the –10 box TAATAT separated by a 17 bp spacer. A comparison of the promoters of all *sr1* homologues revealed that all of them have –35 and –10 boxes separated by a 17 bp spacer region (Figure 2). The only exception is *Brev. brevis* p_{sr1}, which has an 18 bp spacer. All –10 boxes in the *B. cereus* group display the sequence TAAAAT, whereas in all other cases, either TAATAT (as in *B. subtilis*) or TATTAT is found, and, again, in *Brev. Brevis* deviantly TAAGAT. All –35 boxes have the consensus sequence TTGACD with D being A, G or T. The putative transcription start site is always an A, except in *B. pumilus*, where it is G.

Furthermore, in all instances, two BSs for CcpN that represses transcription of *sr1* under glycolytic conditions (17) are present in nearly the same location as in *B. subtilis*. The two BSs for CcpN are located 6–9 bp upstream of the –35 box (3' end of site I) and in the spacer of the –10 box of p_{sr1}. Only *Brev. brevis* BS I is located 19 bp upstream of the –35 box. Whereas in all cases, BS II is located in the 3' half of the p_{sr1} spacer and overlaps at the most the first T of the –10 box, *B. coagulans* BS II overlaps TATT of the –10 box. In the *B. cereus* group and *B. coagulans*, BSs I and II are arranged as inverted repeats, whereas in the *B. subtilis* group and all other species, they are arranged as two direct repeats. No clear definition in this respect is possible for *B. clausii* and *B. halodurans* BSs I and II.

Since CcpA has a minor influence on the glucose-dependent regulation of SR1 transcription, and at least one active CcpA BS (*cre* site) was found upstream of *B. subtilis* p_{sr1} (17), we searched for putative *cre* sites in the vicinity of the *sr1* promoters of all 23 homologues. As shown in Supplementary Figure S4, 21 *sr1* homologues carry at least one hypothetical *cre* site. Thereby, *cre* sites upstream of the –35 box of p_{sr1} were found in 12 cases, and downstream from or overlapping with the transcription start site were found in 19 cases. No putative CcpA BS was found at or in the vicinity of the *Brev. brevis* and at

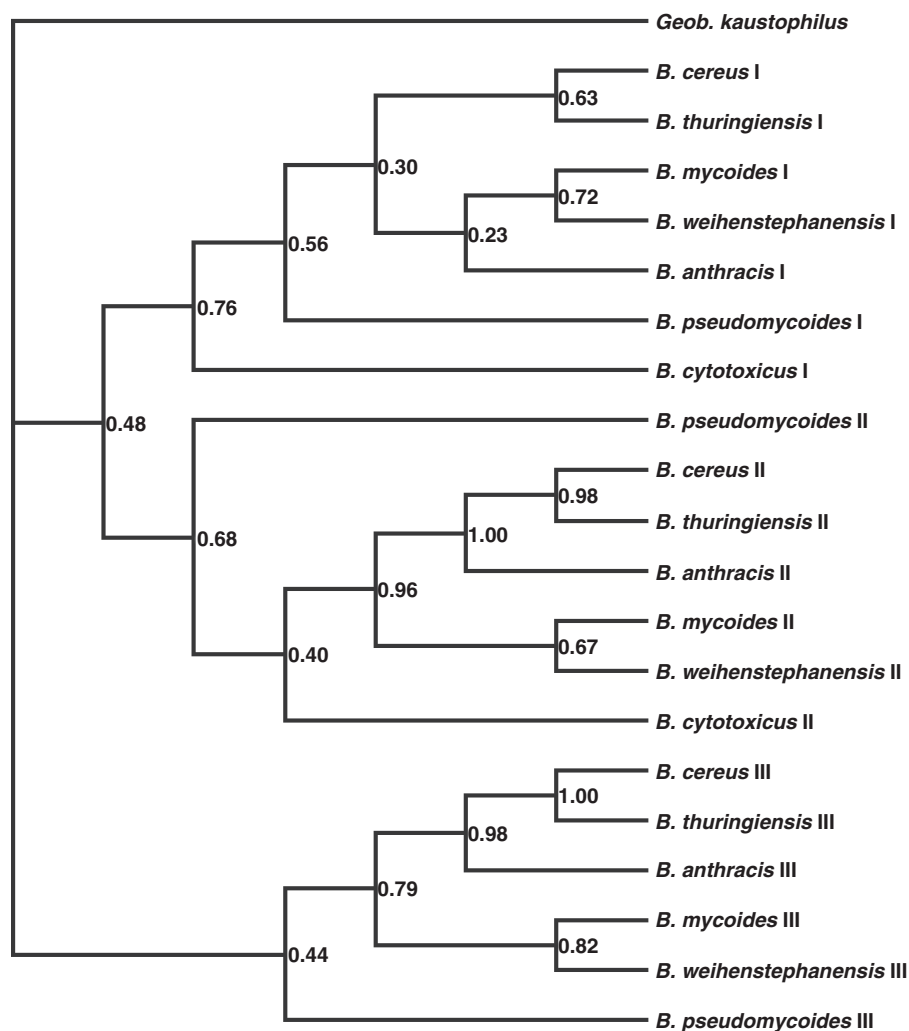


Figure 1. Bayesian phylogeny of the *B. cereus* group SR1 homologues. Our phylogeny suggests that the ancestral gene encoding SR1P was duplicated twice in the ancestor of the *B. cereus* group Bacilli. The first duplication generated copy III and an ancestral sequence for copies I and II. In the second duplication this ancestral sequence was duplicated once more to give rise to the copies I and II. All three copies were retained in subsequent speciation events through which the species of the *B. cereus* group were generated, except for the third copy in *B. cytotoxicus*, which was lost.

the *Geob. kaustophilus sr1* promoters. Since in the majority of cases, *cre* sites are located either within the promoter region (e.g. *bglPH*, *acu*, *amyE*), where they inhibit transcription initiation, or downstream from the transcription start site (e.g. *acsA*, *xyl*, *hut*), where they might block elongation (31), we had shown previously that the *cre* site 275 nt upstream of the transcription start site of *B. subtilis sr1* is active, whereas the *cre* site between nt +12 and +27 is not required (17).

Comparison of the secondary structures/coding properties of the SR1 homologues

The experimentally determined secondary structure of *B. subtilis* SR1 (19) was used to predict the secondary structures of all SR1 homologues. Eight of these predicted secondary structures are shown in Supplementary Figure S5. All SR1 homologues display a large stem-loop (SL1) at their 5' end with a 3–12 nt apical loop and a considerable bulge (13–17 nt) in the 5' half of the stem that

contains the SR1P SD sequence. For *B. subtilis* SR1 SL1, we found that the double-stranded region at the basis of SL1 is required for RNA stability (M. Gimpel, unpublished). In the central part, between SL1 and the terminator stem-loop (TSL), a smaller stem-loop (SL2) is located with 4–7 paired nt and a 5–7 nt loop. The TSLs have a 3–9 nt loop and, except *B. coagulans*, a 12–15 bp stem region. An overview of the terminator sequences is given in Supplementary Table S3. In the *B. cereus* group, three copies of SL1 and SL2 are terminated by a single TSL. All start codons for the SR1P homologues are located in a partially double-stranded region on the 5' half of SL1. All stop codons are located downstream from SL2 near the TSL, but in the *Geobacilli*, a longer sequence separates the stop codon from the TSL, resulting in a slightly longer (225–229 nt) SR1. In the *B. cereus* group, the stop codons of the first two *sr1p* sequences are located upstream of the next SL1, whereas the stop codon of the third copy is located



Figure 2. BSs for CcpN in the promoter regions of *sr1* homologues. The DNA sequences around the promoter regions of the *sr1* homologues are shown. -35 and -10 boxes are in bold and underlined. Putative transcription start sites are shaded in light grey. The two putative BSs for CcpN are indicated in dark grey. The consensus sequence for the CcpN BS is TRTGHYATAYW (27), thereby R = purine, Y = pyrimidine, W = A or T, H = A, C or T.

upstream of the TSL. In the *B. halodurans sr1* gene, the ≈ 1.4 kb long insertion element IS652 is inserted between the stop codon of *sr1p* and the transcription terminator.

Comparison of the SR1P homologues

All SR1P homologues comprise between 37 and 42 aa (Supplementary Figure S6). Interestingly, all members of the *B. cereus* group contain three *sr1p* copies, with the exception of *B. cytotoxicus* that contains two copies. All other species encode only one SR1P. All SR1P aa sequences comprise 3 highly conserved motifs: the N-terminal 7 aa MGTIVCQ, the central FEDEK region and the adjacent VTTLY motif. Furthermore, 3 cysteines at positions 9, 28 and 33 and the isoleucine at position 13 are highly conserved. A comparison of the three *sr1p* copies of the *B. cereus* group peptides shows that copy one is nearly identical in all cases, whereas the second and third copy vary. The first SR1P of all *B. cereus* group members shows 64% identity to the *B. subtilis* SR1P, whereas the last copy is more divergent with only 55–57% identity to *B. subtilis* SR1P. The highest variability can be found in the C-termini of all SR1 peptides. Furthermore, the peptides encoded by *B. megaterium*, *B. halodurans*, *B. pseudofirmus*, *B. clausii*, *B. coahuilensis* and *B. coagulans* reveal more deviations at positions 11–15 and starting from position 26 till the C-terminal end among each other and compared to all other peptides. In contrast, the *Geobacillus* species are similar to each other and more related to the *B. cereus* group peptide I reflecting their position in the phylogenetic tree (Supplementary Figure S3). With 64–71% identity they are more closely related to *B. subtilis* SR1P than the second and third peptides from the *B. cereus* group members (Supplementary Table S3).

Comparison of the complementary regions between the SR1 homologues and the corresponding *ahrC/arg* homologues

An alignment of the coding regions for all *ahrC/arg* homologues is shown in Supplementary Figure S7, whereas Supplementary Figure S8 shows all complementary regions of SR1 and *ahrC* RNA. As highlighted in Supplementary Figure S5, all SR1 homologues experimentally analysed in this study contain between 7 and 11 regions that are complementary to their respective *ahrC* RNA-homologues. Supplementary Table S3 provides an overview of the length of the complementary regions. The location of these regions is more or less conserved, but the primary sequences are highly divergent. An overview of the complementary regions of all 23 SR1 homologues and their target mRNAs that might be involved in base pairing is presented in Supplementary Figure S8. In all cases, the first two complementary regions are found 5' (red) and 3' (green) and overlapping with the base of SL1. The other regions are distributed along the single-stranded regions and the central stem-loop SL2 as in *B. subtilis*. The last complementary region (yellow) is always found at the TSL, either in the 5' part of the stem as in *B. subtilis*, *B. licheniformis*, *B. pumilus*, *Geob. kaustophilus* or at the loop of the TSL as in *B. amyloliquefaciens*, *B. anthracis*, *B. megaterium* and *Geob. kaustophilus*. In *B. subtilis*, this region (designated G) is most important for the initial interaction with the 5' complementary region (G') of the *ahrC* target RNA ≈ 90 bp downstream of the *ahrC* ribosome BS (19). In *B. thuringiensis*, two *ahrC* homologues exist, *arg2* highly similar to *B. subtilis ahrC*, and the more divergent *arg1*. As shown in Supplementary Figure S5, *B. thuringiensis* SR1 is predicted to interact with both *arg* mRNAs using different complementary

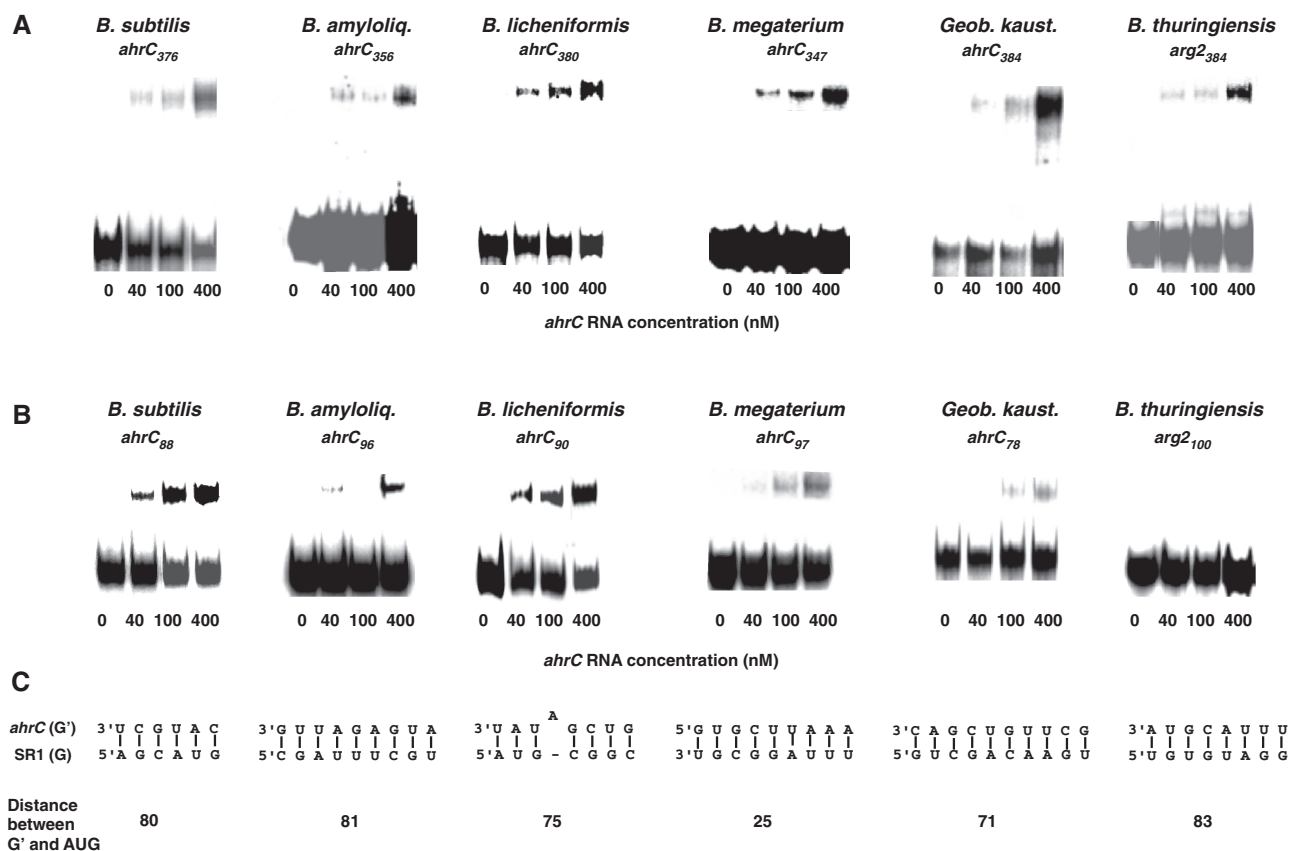


Figure 3. Binding assays of SR1/*ahrC* RNA pairs from different *Bacillus* species. Binding experiments were performed as described in Materials and Methods section. Autoradiograms of gel-shift assays are shown. The concentration of unlabelled *ahrC* species is indicated in nM. (A) Binding assays with homologous SR1/*ahrC* pairs from *B. subtilis*, *B. amyloliquefaciens*, *B. licheniformis*, *B. megaterium*, *Geob. kaustophilus* and *B. thuringiensis* III. SR1 species from these Bacilli were 5' end-labelled with [γ -³²P]-ATP and used at a final concentration of 4 nM (at least 10-fold lower concentration than *ahrC* RNA) in all experiments. *ahrC*-RNA species of the indicated length comprising the central part of *ahrC* with all complementary regions (Supplementary Figures S7 and S8) were used. (B) Binding assays with homologous SR1/*ahrC* pairs as above. *ahrC* RNAs containing only region G' were paired with the SR1 homologues comprising all complementary regions. (C) Regions that can base pair in the experiment shown in (B). Below, the distance between the 5' end of region G' and the 3' end of the corresponding *ahrC* start codons is shown for each *ahrC* RNA/SR1 pair.

regions. The interaction pattern for SR1/*arg2* is similar to the interaction patterns of the other SR1 homologues with their respective *ahrC/arg* genes. In contrast, the interaction pattern for SR1/*arg1* involves the central instead of the base regions of SL1. *B. anthracis* encodes only *arg2*, and the *arg2*/SR1 interaction pattern resembles that of the *B. thuringiensis arg2*/SR1 pattern.

Binding assays of SR1/*ahrC* mRNA pairs

To analyse the predicted interactions of SR1 homologues with their cognate *ahrC* mRNAs experimentally, *in vitro* binding studies were performed for the SR1/*ahrC* RNA pairs of *B. subtilis*, *B. amyloliquefaciens*, *B. licheniformis*, *B. megaterium*, *Geob. kaustophilus* and *B. thuringiensis*. *B. halodurans* and *B. pumilus* were not included, because the *sr1* gene in *B. halodurans* is interrupted by IS652 and did not yield a distinct SR1 species in northern blots, and *sr1* is apparently not expressed in *B. pumilus* (see below and Figure 4). For *B. thuringiensis*, *in vitro* transcribed first, second and third copies of SR1 were analysed separately, since RNA/RNA complexes formed with species larger than 400 nt do not run into native gels. SR1

species were generated *in vitro* using T7 RNA polymerase, 5' end-labelled, gel-purified and used for binding assays with unlabelled *ahrC*-RNA species of about 350–380 nt comprising all predicted regions for base pairing (Supplementary Figure S8). *B. thuringiensis* SR1 I and SR1 II did not form complexes with *arg2* RNA (not shown). In all other cases, SR1/*ahrC* RNA complexes were formed (Figure 3A), albeit with varying efficiencies. The most efficient interactions were observed for *B. subtilis*, *B. licheniformis* and *Geob. kaustophilus*, where at the highest *ahrC* RNA concentration between 30% and 42% of labelled SR1 was bound, whereas in the other cases, only $\approx 10\%$ of SR1 were bound. These differences might be due to differences in number and/or accessibility of the complementary regions or the requirement of additional helper proteins for complex formation *in vivo*. Previously, we have shown in *B. subtilis* that the initial contact between SR1 and *ahrC* RNA requires complementary region G (19). This region is located in the 5' half of the SR1 TSL downstream of the coding region for SR1P. The complementary region G' is found about 90 nt downstream of the *ahrC* RBS (ribosome binding site). In *B. subtilis*, SR1 binds to this region and induces

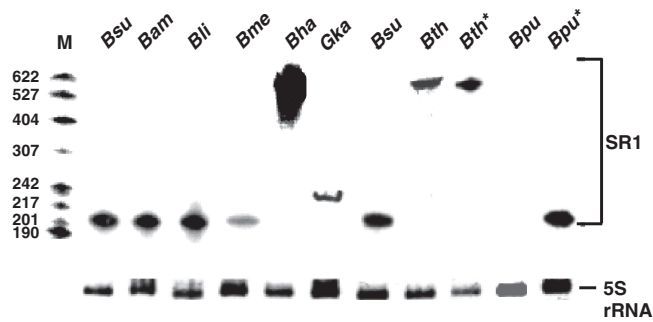


Figure 4. Expression of SR1 in eight *Bacillus/Geobacillus* species. All strains were grown as described in Materials and Methods section. At the onset of stationary growth phase, samples were withdrawn, total RNA prepared and subjected to NB. For hybridization, [α - 32 P] dATP-labelled DNA probes for the respective SR1 homologues were used. To compare the amounts of RNA loaded onto the gel, signals for 5S rRNA obtained by ethidium-bromide staining are shown. In the case of *B. thuringiensis* and *B. pumilus*, the *sr1* gene was expressed in parallel from a high-copy vector (pWSR1/M60 and pWSR1/M56; Supplementary Table S2) in *B. subtilis* (lanes labelled with asterisk) and loaded next to the total RNA isolated from the original host.

structural changes \approx 40–60 nt downstream of the RBS that prevent initiation of *ahrC* translation (19, see model in Supplementary Figure S11). Therefore, we investigated if *ahrC* RNA species of the other Bacilli that comprise only region G' could be bound by the cognate SR1 species. Complexes with this short *ahrC* RNA (*arg2* in *B. thuringiensis*) were observed for *B. subtilis*, *B. amyloliquefaciens*, *B. licheniformis*, *B. megaterium* and *Geob. kaustophilus* but not for *B. thuringiensis* SR1 III (Figure 3B). One explanation for the failure of SR1 III to bind to *arg2*-G' might be that *in vivo* the interaction partner of *arg2* is full-length (587 nt) *B. thuringiensis* SR1, whose structure differs from the short species used in these experiments. However, due to technical constraints, we could not investigate such a long sRNA in the binding assays (see above). Predicted interactions with *B. thuringiensis* SR1 and *arg1* mRNA that does not exist in *B. subtilis*, could not be confirmed in binding assays with SR1/*arg1* species comprising all complementary regions. Therefore, it is not clear if this predicted interaction is relevant.

In the binding assays, the region located next to the *ahrC* SD sequence was used as region G' (Figure 3C). At primary sequence level, there is no conservation in regions G and G' among the SR1 and *ahrC* homologues (see above and Supplementary Figures S2 and S8). Even the distance between the *ahrC* start codon and G' and the GC-content of G/G' vary (Supplementary Figures S8). In the cases analysed experimentally, the distance between G' and *ahrC* start codon was between 25 nt and 83 nt. The G/G' double-strand comprised between 6 and 10 contiguous bp that were in one case interrupted by one bulged-out nucleotide. In the majority of the SR1 species, G is located either at the 5' arm of the terminator stem as in *B. subtilis*, *B. licheniformis* and *B. pumilus* (Supplementary Figures S2, S5), and would need *in vivo* an enzyme to open up the double-stranded region as proposed previously (19).

In other cases, G is located at the terminator loop (*B. amyloliquefaciens*, *B. megaterium*, *Geob. kaustophilus* and *B. thuringiensis*) and is in *B. thuringiensis* and *Geob. kaustophilus* preceded by a second complementary region in the 5' half of the stem.

The results of the *in vitro* binding assays suggest that the repression of *ahrC* translation by SR1 is conserved, and that—as previously found in *B. subtilis*—the G/G' base pairing is—despite all variability—sufficient to initiate binding.

Both regulation of *ahrC* translation and *gapA* mRNA stability occur in stationary growth phase. Therefore, the question arises if *sr1p* translation and SR1/*ahrC* base-pairing interfere. On the one hand, in all SR1 homologues, between one and four complementary regions are located downstream from the translated region (Supplementary Figures S2, S5 and S8), and in five *Bacillus* species SR1/*ahrC* RNA-complexes could form when only one of these complementary regions was present (Figure 3). However, it cannot be excluded that complementary regions B–F, which were previously shown to have only a marginal effect on the SR1/*ahrC* interaction in *B. subtilis* (19), have a higher impact on *ahrC* RNA binding in the other SR1 homologues. As these regions overlap with the *sr1p* ORF, binding of B to F might hinder *sr1p* translation. On the other hand, the *sr1p* ORF is poorly translated, as a translational *sr1p-lacZ* fusion did not yield measurable β -galactosidase activities in *B. subtilis* (17), and only the addition of a 3xFLAG tag allowed to visualize SR1P in western blots (22). However, taken together, the mutual interference of the two SR1 functions cannot be entirely excluded.

Since the primary sequences of the regions in *ahrC* or *arg*, which are required for the initial interaction with homologous SR1 species are highly different, it cannot be assumed that heterologous SR1 species are able to complement a Δ *sr1* *B. subtilis* strain for the effect on AhrC, and, thus, the *rocABC* and *rocDEF* operons.

Identification of SR1 homologues in eight different species in northern blots

For a comparative experimental analysis of SR1 homologues, nine species were chosen: *B. subtilis*, *B. amyloliquefaciens*, *B. licheniformis*, *B. pumilus* (the first three belonging to the *B. subtilis* group, the latter one closely related), *B. thuringiensis* and *B. anthracis* (*B. cereus* group) and the three ungrouped *B. halodurans*, *B. megaterium* and *Geob. kaustophilus*. All strains except *B. anthracis* were grown in TY complex medium under the appropriate growth conditions (see Materials and Methods section), RNA isolated and subjected to NB with the respective probes. SR1 homologues from *B. subtilis*, *B. amyloliquefaciens* and *B. licheniformis* were detected with a probe against *B. subtilis* SR1 (Figure 4). For the other SR1 species, the cognate probes were used. As predicted, SR1 from *Geob. kaustophilus* is with 229 nt larger in size than the *B. subtilis*, *B. amyloliquefaciens*, *B. licheniformis* and *B. megaterium* SR1 homologues. Interestingly, in *B. halodurans*, a mixture of SR1 species of different lengths between 400 nt and 650 nt was

Table 1. β -galactosidase activities of wild type and *cepN* knockout strains

lacZ fusion	β -galactosidase activity (Miller units) in						
	DB104 (–Glc)	DB104 (+Glc)	GRF	<i>AccpN</i> (–Glc)	<i>AccpN</i> (+Glc)	GRF	<i>F</i>
pACT87 <i>Bsu</i>	2282 ± 171	205 ± 39	11.1	2181 ± 146	1453 ± 156	1.5	1.0
pACS54 <i>Bli</i>	1743 ± 34	129 ± 15	13.6	1687 ± 180	961 ± 95	1.8	1.0
pACS55 <i>Bam</i>	1567 ± 65	77 ± 19	20.4	1584 ± 111	983 ± 105	1.0	1.0
pACS56 <i>Bth</i>	4169 ± 88	428 ± 23	9.7	4224 ± 32	3736 ± 71	1.0	1.0
pACS57 <i>Bpu</i>	1785 ± 40	158 ± 23	11.3	2510 ± 139	2020 ± 195	1.2	1.4
pACS58 <i>Bha</i>	216 ± 19	22 ± 3	9.7	998 ± 127	526 ± 54	1.9	4.6
pACS59 <i>Bme</i>	223 ± 21,5	30 ± 14	7.4	809 ± 80	512 ± 76	1.6	3.6
pACS60 <i>Ban</i>	2341 ± 117	146 ± 22	16.3	2440 ± 126	2315 ± 38	1.1	1.0
pACS61 <i>Gka</i>	1714 ± 113	160 ± 36	10.7	1681 ± 106	1350 ± 21	1.2	1.0
pACS62 <i>Bsu</i> C	2300 ± 57	206 ± 11	11.2	2135 ± 18	1687 ± 76	1.3	0.9
pACS63 <i>Bsu</i> P	2196 ± 74	1590 ± 71	1.4	2042 ± 79	1496 ± 127	1.4	0.9
pACS64 <i>Bha</i> C	270 ± 14	58 ± 18	4.7	1100 ± 44	666 ± 10	1.7	4.0
pACS65 <i>Bha</i> P	1934 ± 1	1182 ± 166	1.7	1895 ± 47	1491 ± 26	1.3	1.3
pACS66 <i>Bme</i> C	322 ± 2.1	49 ± 34	6.7	1052 ± 62	522 ± 36	2.0	3.3
pACS67 <i>Bme</i> P	1736 ± 80	1582 ± 7	2.0	1571 ± 77	1611 ± 43	1.0	0.9

Bsu, *B. subtilis*; *Bli*, *B. licheniformis*; *Bam*, *B. amyloliquefaciens*; *Bth*, *B. thuringiensis*; *Bpu*, *B. pumilus*; *Bha*, *B. halodurans*; *Bme*, *B. megaterium*; *Ban*, *B. anthracis*; *Gka*, *Geob. kaustophilus*. All pAC derivatives contain the promoter, both CcpN sites and about 67 more upstream bp. Cultures were grown in SP medium with 2% or without glucose. All values represent averages of at least three independent determinations with five transformants grown in parallel; GRF, glucose repression factor, the ratio between the values obtained without and with glucose in wild-type DB104 and DB104 (*AccpN::phleo*), respectively. *F*, ratio of the values obtained for *AccpN* and DB104 without glucose. A value >1 suggests a glucose-independent repression by CcpN. Lower part: C, pAC derivative comprises promoter and both CcpN BS, but no further upstream sequences; P, pAC derivative contains only the promoter and CcpN BS II, but lacks BS I (Figure 2).

observed, which apparently results from unspecific termination of *sr1* transcription within insertion element IS652.

In *B. thuringiensis*, a \approx 580 nt long species encoding the three SR1P peptides was expressed. To exclude that a processing into smaller SR1 species escaped our attention, we performed primer extension and 3' RACE experiments using primers complementary to different SR1 regions. Primer extension with primers located within each of the three *sr1p* regions resulted in a single clear signal corresponding to the 5' end of a 587 nt RNA (Supplementary Figure S9). 3' RACE yielded the predicted 3' end of a 587 nt SR1 as well as signals representing various degradation products, which were evenly distributed and did not indicate specific processing sites. Therefore, the triplicate SR1 of *B. thuringiensis* is not processed into three shorter species.

Although high amounts of total RNA were isolated from *B. pumilus*, the corresponding SR1 homologue could not be detected in northern blots with the cognate SR1 probe. The expression of *B. megaterium sr1* was weaker than that of the other sRNAs. One reason could be transcriptional down-regulation of this RNAs in its native host. This result prompted us to analyse the strength of the nine different SR1 promoters.

Experimental analysis of the promoter strength and the role of CcpN for nine selected SR1 species

To this end, transcriptional *lacZ*-fusions were constructed comprising 87 bp upstream of the –35 box and 10 nt downstream from the putative transcription start sites containing both CcpN BSs and about 40 nt upstream of them and integrated into the *amyE* locus of the chromosome of *B. subtilis* strains DB104 and

DB104 (*AccpN::phleo*). The latter strain was used to investigate the effect of CcpN, i.e. transcription repression in the presence and absence of CcpN under glycolytic conditions (17). Cultures were grown in SP medium with and without 2% glucose and β -galactosidase activities determined. In the absence of glucose, activities were high (between 1567 MU and 4169 MU) for all *sr1* promoters except those of *B. halodurans* and *B. megaterium* (Table 1). In all cases, in the presence of 2% glucose, \approx 7–20-fold lower β -galactosidase activities were determined in DB104. This result confirms that the two CcpN BSs found in nearly the same locations as in *B. subtilis* p_{sr1} are active. In the absence of CcpN, the β -galactosidase activities were—except for *B. halodurans* and *B. megaterium*—in the same range as in the absence of glucose, verifying that CcpN is responsible for this effect. In *B. halodurans* and *B. megaterium*, the promoter strength was \approx 10-fold lower in the absence of glucose compared to the other species, but increased about 3.6–4.6-fold when CcpN and glucose were not present. This result suggests in these two species an additional glucose-independent repression by CcpN, which has not been reported so far. Surprisingly, a small (1.5–1.9-fold) but distinctive glucose repression was still observed in the absence of CcpN in *B. subtilis*, *B. licheniformis*, *B. halodurans* and *B. megaterium*. Since none of the constructed plasmids contained a *cre* site (Supplementary Figure S4), this residual glucose repression cannot be attributed to CcpA, but must be due to another, still unknown glucose-dependent factor.

To corroborate that indeed CcpN was responsible for the unanticipated results obtained with *B. halodurans* and *B. megaterium*, six additional pAC derivatives were

constructed. Three of them contain only the p_{sr1} region with CcpN BS II, but lack BS I upstream of the -35 box in *B. subtilis* (pACS63), *B. halodurans* (pACS65) and *B. megaterium* (pACS67). The other three contain the *sr1* promoters with only the two CcpN BSs, but without further upstream sequences (pACS62, pACS64 and pACS66 for *B. subtilis*, *B. halodurans* and *B. megaterium*, respectively). The measured β -galactosidase activities (Table 1) indicate that the three promoters without CcpN BS I have almost the same strength (1500–2000 MU) as one would expect from the nearly identical sequences of their -35 and -10 boxes. However, as soon as two CcpN BSs were present, the promoter activity decreased to the values obtained with the longer constructs (Table 1) under non-glycolytic conditions. Although a certain degree of CcpN-dependent, glucose-independent repression was found *in vivo* at the *gapB* and *pckA* promoters in *B. subtilis* (32), and at all three promoters *in vitro* (20), we did not observe such a repression *in vivo* at p_{sr1} . Since the location of the CcpN BS is identical at all *sr1* promoters in contrast to their location at the *gapB* and *pckA* promoters, where BS I overlaps the -10 box and BS II the region around $+20$, this cannot be the reason for the observed differences. A comparison of the nt sequence of CcpN BS I for all *sr1* promoters analysed in this report reveals a difference in two apparently critical nt: HY of the consensus sequence TRTGHYATAYW is in all cases analysed experimentally TT, TC (in *B. pumilus*) or AT (in *Geob. kaustophilus*), whereas it is AC in *B. megaterium* and *B. halodurans*. Therefore, we hypothesize that the glucose-independent repression at these two promoters is due to a more efficient binding of CcpN at BS I. However, the 1.5-fold higher values in the $\Delta ccpN$ strain (-glucose) in the absence of BS I compared to the presence of BS I suggest the additional binding of a yet unknown glucose-independent regulator in this region. The 1.7- and 2.0-fold glucose-dependent transcriptional repression also observed with these shorter fusions in the absence of both CcpN and any *cre* sites points to a supplementary small effect of an unknown glucose-dependent regulator (see above). Future research will be aimed at the identification of this factor.

Ability of 11 SR1P homologues to stabilize *B. subtilis* *gapA* RNA and to interact with *B. subtilis* GapA protein

As shown previously by NB, *gapA* operon mRNA is barely detectable in an SR1 knockout strain after growth in complex medium till onset of stationary phase (22). Inducible overexpression of wild-type SR1 encoding SR1P from a multicopy vector can complement this defect, leading to stabilization and, as a consequence, visualization of *gapA* mRNA. SR1P interacts with GapA protein, and this interaction stabilizes *gapA* mRNA by a hitherto unknown mechanism (22). To analyse the ability of SR1P homologues to stabilize *B. subtilis* *gapA* mRNA, *sr1* homologues from *B. amyloliquefaciens*, *B. licheniformis*, *B. pumilus*, *B. thuringiensis*, *B. anthracis*, *B. halodurans*, *B. megaterium*

and *Geob. kaustophilus* were inducibly overexpressed in *B. subtilis* ($\Delta sr1::cat$) under control of the *tet* operator. All SR1P homologues were tagged at the C-terminus with a Strep tag followed by the *B. subtilis* SR1 transcription terminator. In the case of *B. thuringiensis*, three plasmids were constructed, each of them encoding one of the three different peptides SR1/P1, P2 and P3 (Figure 5 and Supplementary Figure S6). Cells were grown in TY medium until onset of stationary phase, induced with anhydro-tetracycline for 15 min, harvested, and RNA was isolated and subjected to NB. In spite of their differences in the aa sequences, 10 of 11 SR1P homologues were able to complement the absence of *B. subtilis* SR1P (Figure 5A and D) i.e. to stabilize *gapA* mRNA. Only *B. megaterium* SR1P was not functional. The expression and *gapA* stabilizing function of the entire *B. thuringiensis* *sr1* gene encoding the three peptides was analysed, too. It resulted in a ≈ 580 nt long sRNA in northern blots, which is the size of an unprocessed SR1 RNA (Figure 5A) and was as functional in complementation of the *sr1* knockout strain as each single *sr1P* encoding region.

To investigate whether the SR1P homologues were able to interact with *B. subtilis* GapA, the strains were cultivated as above, induced, cells harvested, protein extracts prepared and loaded onto a streptactin column as described (22). Elution fractions were analysed on SDS-Tris-glycin-PAA gels for co-elution of *B. subtilis* GapA (Figure 5B). Interestingly, only in the presence of four SR1P homologues—*B. subtilis*, *B. amyloliquefaciens* and *Geob. kaustophilus* SR1P as well as *B. thuringiensis* SR1P/P1 (which is identical to P1 from *B. anthracis*)—*B. subtilis* GapA was co-eluted (Figure 5B). In the other cases, GapA was detected in the washing fractions by western blotting (as shown for *B. halodurans* and *B. megaterium* SR1P (Figure 5C) indicating that its interaction with the heterologous SR1P was weaker than with *B. subtilis* SR1P. Apparently, with the exception of *B. megaterium* SR1P, even the weak interactions were sufficient for a stabilizing effect on *B. subtilis* *gapA* mRNA *in vivo* as detected in the northern blots. The overview of the co-elution data in conjunction with the corresponding SR1 peptide sequences (Figure 5D) reveals that two regions of SR1P differ markedly in those peptides that were impaired in GapA binding: the EAIHY region (aa 11–15) and the VTTLY (aa 21–25) region, which are separated by the highly conserved FEDEK motif. As we have shown previously, the highly heterogenous C-terminus is not important for SR1P function, as the C-terminal 9 aa of *B. subtilis* SR1P can even be deleted without functional consequences (22). The highly divergent regions might contain candidate aa for the interaction surface with GapA. An alignment of the aa sequences of the corresponding 23 GapA proteins is shown in Supplementary Figure S10. All GapA proteins display between 85% and 97% identity on aa level with *B. subtilis* GapA, except for the *B. cereus* group members that show 80% identity.

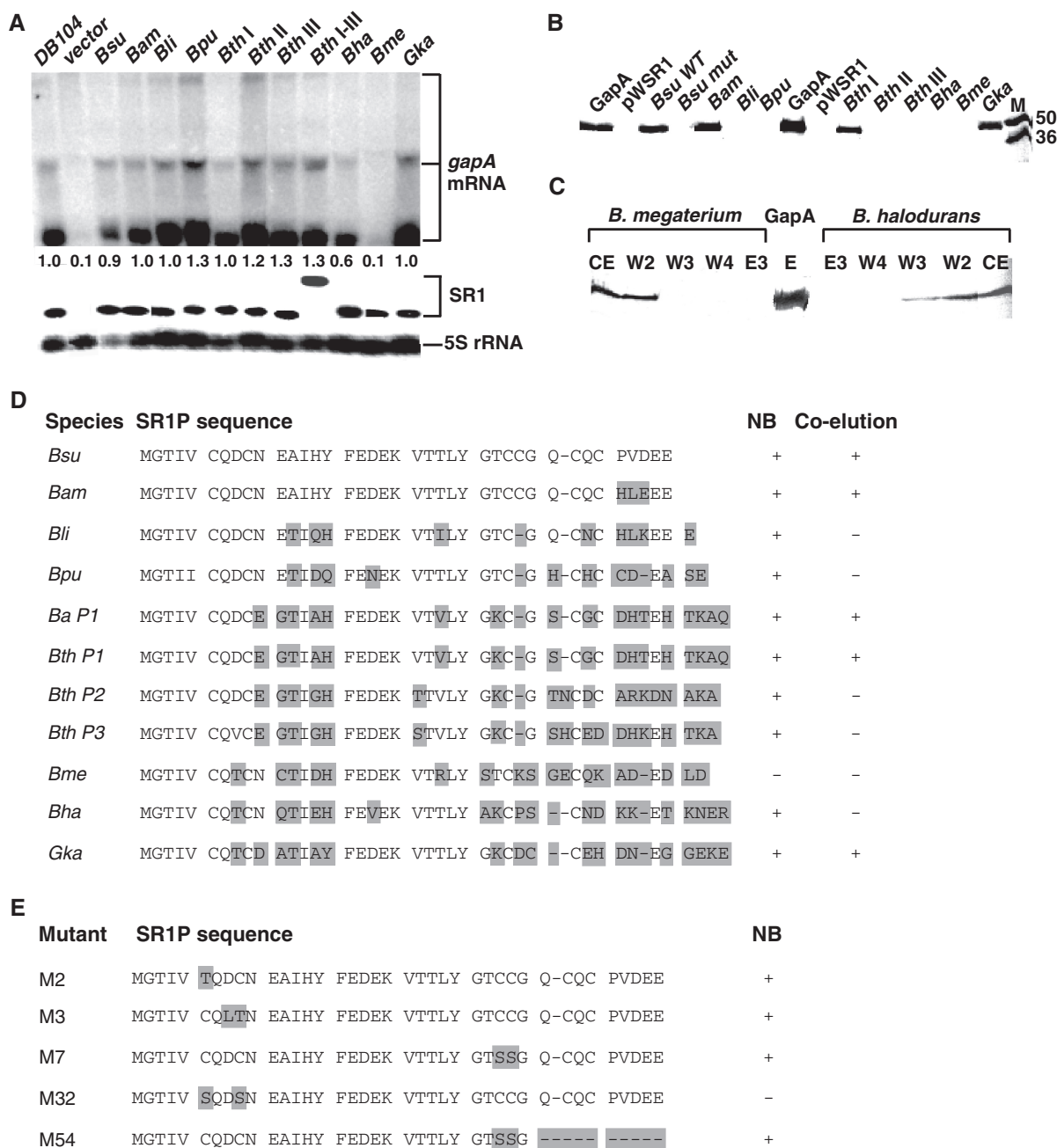


Figure 5. Comparative analysis of SR1 homologues in northern blots and co-elution experiments. (A) Northern blots. *Bacillus subtilis* strains were grown under the appropriate conditions in TY medium (see Results section) until the onset of stationary phase, samples taken, total RNA prepared, treated with glyoxal, separated on 1.5% agarose gels, blotted onto nylon membrane and hybridized with a [α - 32 P] dATP-labelled DNA probe for *B. subtilis gapA* (three species of 1.2kb, 2kb and 6kb) and re-probed with specific [α - 32 P] dATP-labelled DNA probes for the respective SR1 homologues. For the correction of loading errors, filters were re-probed with a [γ - 32 P]-ATP-labelled oligonucleotide specific for 5S rRNA (Supplementary Table S1). Wild type, *B. subtilis* strain DB104. All the other strains are DB104 (*Asr1::cat*) containing either an empty vector or the vector with the corresponding *sr1* gene. In the case of *B. thuringiensis sr1*, four vectors were analysed expressing the first, the second or the third copy of *sr1p* (I, II or III) or the entire *sr1* gene with all three *sr1p* copies (I-III) (Supplementary Figures S5 and S6). The numbers below the gel indicate the relative amounts of *gapA* mRNA calculated by using the loading control (signal for 5S rRNA). (B) Co-elution experiments. Nine SR1P homologues were expressed with a C-terminal Strep tag (tag not shown in the sequence) from a tet-inducible promoter on the corresponding multicopy vector pWSR1/MX (Supplementary Table S2) in *B. subtilis* strain DB104 (*Asr1::cat*). The ability of each SR1P homologue to tightly bind and co-elute *B. subtilis* GapA was investigated in a co-elution assay with a streptactin column as described previously (22). Plasmid pWSR1 expresses *sr1* without Strep tag. Bsu mut expresses a mutated *sr1* which is not functional in stabilization of *gapA* mRNA in northern blots. An aliquot of each elution fraction E3 was separated on a 17.5% SDS-Tris-glycine PAA gel along with purified GapA and a size marker (M) in kD and stained with Coomassie blue. (C) Western blot analysis of *B. halodurans* and *B. megaterium* SR1P flow-through, washing and elution fractions as an example for a very weak interaction with the heterologous *B. subtilis* GapA. Here, GapA is already visible in the washing fractions. (D) Overview of the complementation of *B. subtilis* *Asr1p* by 10 different SR1P homologues. On the one hand, the ability of each SR1 homologue to complement a *B. subtilis* *sr1* knockout strain by stabilizing the *gapA* mRNA was analysed by NB (see (A)). On the other hand, the ability of the SR1P homologues to interact with *B. subtilis* GapA was investigated by a co-elution assay (see (B)). +, complementation in northern blot/co-elution of *B. subtilis* GapA, -, no complementation/co-elution. Ba (*B. anthracis*) P1 is identical to Bth P1. (E) Overview of the complementation of *B. subtilis* *Asr1p* by five *B. subtilis* SR1P mutants with substituted or lacking cysteine residues.

Role of Cysteine residues in SR1P

To analyse the importance of the six cysteine residues for the ability of SR1P to stabilize *gapA* mRNA, mutants M2 (C6T), M3 (D8L, C9T), M7 (C28S, C29S), M32 (C6S, C9S) and M54 (C28S, C29S and Δ 31-39) were analysed in NB. The results with mutants M7 and M54 (Figure 5E) show that the four C-terminal cysteine residues C28, C29, C32 and C34 are not necessary for the function of SR1P in *gapA* stabilization. However, whereas a single substitution of C6 nor C9 could be tolerated (M2, M3), a double substitution (M32) abolished the functionality of SR1P. This indicates that at least one of the N-terminal cysteine residues—C6 or C9—is required. Additionally, to rule out that the six cysteine residues in wild-type SR1P form a Zn finger motif that coordinates Zn^{2+} , we analysed the functionality of SR1P in the presence of EDTA, a chelator for divalent cations. To this end, three co-elution experiments were performed in parallel with crude protein extracts from DB104 (*Δsr1:cat*, pWSR1/M25) in the presence of either 50 mM EDTA, 0 mM EDTA or 1 mM $ZnCl_2$. The chelator and $ZnCl_2$ were added after sonication and before loading the extracts onto the streptactin columns. No differences between the amounts of co-eluted GapA were observed (not shown), indicating that SR1P is not a Zn finger protein.

CONCLUSIONS

So far, only a few studies have been published that deal with the computational search for sRNA homologues and their experimental investigation. These concern sRNAs restricted to Gram-negative bacteria, mostly enterobacteriaceae: SgrS (30, 33), GlmY/GlmZ (34) and GcvB (35).

Here, we present the first analysis for an sRNA from Gram-positive bacteria. We identified 23 homologues of the dual-function sRNA SR1 in *Bacillus*, *Geobacillus*, *Anoxybacillus* and *Brevibacillus* species. No homologues were found in other bacteria, neither Gram-positive nor Gram-negative ones. Hence, SR1 originated between 0.9 and 1.3 billion years ago as this is the timescale in which the species encoding SR1 diverged (36). The expression of all *sr1* homologous genes is under control of transcriptional repressor CcpN, which binds at nearly the same positions at all *sr1* promoters. Although the promoters of the tested nine homologues were active and all but those of *B. halodurans* and *B. megaterium* were of similar strength in *B. subtilis*, SR1 could not be detected in total RNA isolates from *B. pumilus*. This suggests that a still unknown, species-specific regulator might control *sr1* expression in *B. pumilus*. Furthermore, a so far unprecedented glucose-independent 3–4-fold repression of *sr1* transcription by CcpN was observed in *B. halodurans* and *B. megaterium*. Interestingly, different contributions of σ^{54} and σ^{70} and a two-component system (TCS) to the transcription of GlmY/Z homologues from different species were found (31). Thus, other regulatory principles might be also used for *sr1* homologues, which were not included in this experimental study.

All homologues encode both highly similar SR1P peptide homologues of 37–42 aa and contain 7–11 short

regions complementary to the cognate coding regions of *ahrC/arg*. On primary sequence level, the peptide-encoding regions are more conserved than the base-pairing regions. However, on structural level, the location and length of the complementary regions as well as their ability to base pair with *ahrC* mRNA, is also conserved (Figure 3 and Supplementary Figures S2, S5 and S8). As previously found in *B. subtilis*, the G/G' base pairing is sufficient in most cases to initiate binding between SR1 and *ahrC* mRNA (for a model, see Supplementary Figure S11). This suggests that the inhibition of *ahrC/arg* translation is also conserved. An interference of SR1P synthesis and SR1/*ahrC* mRNA base pairing cannot be entirely excluded, although the translational efficiency of *sr1p* is very low, and the regions decisive for the initial interaction are located downstream of the *sr1p* stop codon.

Our results are in contrast to those of Horler and Vanderpool (30) who found that the base-pairing function of SgrS is more conserved than the peptide-encoding function. The species that encode SgrS/SgrR diverged between 0.4 and 0.7 billion years ago (36). Recently, a functional homologue of SgrS, TarA, which regulates *ptsG* was discovered in *Vibrio cholerae*. In contrast to SgrS, TarA is smaller (100 nt versus 227 nt), does not contain the 43 aa SgrT ORF and is not downregulated by SgrR but upregulated by transcription activator ToxT (37). TarA escaped the computational approach by Horler and Vanderpool, because they used as search criteria the neighbourhood of *sgrS* and *sgrR* encoding its *E. coli* regulator, which is conserved in a variety of Gram-negative bacteria. Presently, we cannot exclude that in non-related bacteria SR1 functional homologues exist that are either controlled by other transcription factors or whose SR1P sequences differ significantly from those analysed here. Since CcpN is encoded in a number of firmicutes (32), among them *Staphylococcus aureus*, *Enterococcus faecalis* or *L. monocytogenes*, we used *S. aureus* as an example to search for peptides comprising 20–50 aa in the vicinity of whose encoding genes/promoters is at least one CcpN BS with no more than one deviation from the *B. subtilis* consensus. However, none of the peptides found by this search showed any similarity on aa level to SR1P. The same was true for all other peptides of this size range predicted in *S. aureus* with our programme. This is not too surprising, because the GapA proteins of *B. subtilis* and *S. aureus* share only 53% aa identity compared to at least 80% identity between the GapA proteins of the 23 analysed Bacilli. Given that all these peptide homologues must bind their homologous GapA proteins, it is difficult to imagine a high similarity on aa level between peptides of less-related species. However, the discovery of 23 homologous SR1P will contribute to the elucidation of interacting regions/residues between SR1P and GapA. Once this region is identified, new bio-computational tools can be developed to search for functional SR1P homologues in distantly related bacteria.

Strikingly, all *B. cereus* group members, which contain more than one *sr1p* copy, are pathogens. Why do all these pathogens contain two or three *sr1p* copies? Recently, it

has been proposed by Papenfort *et al.* that conserved sRNAs with seemingly unrelated functions constitute a reservoir of regulators that act to tame foreign genes and to integrate them into existing regulatory networks (38). Alternatively, the pool of already existing regulators might be expanded in order to regulate virulence genes. It is tempting to speculate that the two duplications of *sr1p* in the *B. cereus* group are such an enlargement that might allow these pathogens to adapt to the adverse environment of their hosts.

In summary, there are many commonalities between the 23 SR1 homologues showing that the two functions have been remarkably conserved during 0.9–1.3 billion years of evolution. This timescale is much longer than the time of conservation for SgrS for which only one of the two functions, the base-pairing function, was maintained during the whole evolution of this sRNA. This demonstrates the importance of SR1. Nevertheless, there are some interesting differences between the members of the SR1 family in transcriptional regulation as well as the gene duplications in the pathogenic *B. cereus* group, which are subjects for further research.

SUPPLEMENTARY DATA

Supplementary Data are available at NAR Online: Supplementary Tables 1–3 and Supplementary Figures 1–11.

ACKNOWLEDGEMENTS

The authors thank S. Pohl (Newcastle), who performed the two PCR reactions from the *B. anthracis sr1* upstream and coding regions and sent us the gel-purified fragments. We are grateful to R. Borriss (Berlin), G. Steinborn (Gatersleben), R. Biedendieck (Braunschweig), M. Miethke (Marburg), and S. Graf (Mainz) for sending us the *B. amyloliquefaciens* FZB42, *B. licheniformis* ATCC14580, *B. megaterium* DSM319, *B. halodurans* DSM497 and *Geob. kaustophilus* DSM7263 strains, respectively.

FUNDING

Deutsche Forschungsgemeinschaft [Br1552/6-3 to S.B.]. Funding for open access charge: Deutsche Forschungsgemeinschaft DFG.

Conflict of interest statement. None declared.

REFERENCES

- Gottesman, S. and Storz, G. (2011) Bacterial small RNA regulators: versatile roles and rapidly evolving variations. *Cold Spring Harb. Perspect. Biol.*, **3**, pii: a003798.
- Brantl, S. (2009) Bacterial chromosome-encoded small regulatory RNAs. *Future Microbiol.*, **4**, 85–103.
- Irnov, K., Sharma, C.M., Vogel, J. and Winkler, W.C. (2010) Identification of regulatory RNAs in *Bacillus subtilis*. *Nucleic Acids Res.*, **38**, 6637–6651.
- Rasmussen, S., Nielsen, H.B. and Jarmer, H. (2009) Transcriptionally active regions in the genome of *Bacillus subtilis*. *Mol. Microbiol.*, **73**, 1043–1057.
- Toledo-Arana, A., Dussurget, O., Nikitas, G., Sesto, N., Guet-Revillet, H., Balestrino, D., Loh, E., Gripenland, J., Tiensuu, T., Vaitkevicius, K. *et al.* (2009) The *Listeria* transcriptional landscape from saprophytism to virulence. *Nature*, **459**, 950–956.
- Geissmann, T., Chevalier, C., Cros, M.-J., Boisset, S., Fechter, P., Noirot, C., Schrenzel, J., François, P., Vandenesch, F., Gaspin, C. *et al.* (2009) A search for small noncoding RNAs in *Staphylococcus aureus* reveals a conserved sequence motif for regulation. *Nucleic Acids Res.*, **37**, 7239–7257.
- Bohn, C., Rigoulay, C., Chabelskaya, S., Sharma, C.M., Marchais, A., Skorski, P., Borezée-Durant, E., Barbet, R., Jacquet, E., Jacq, A. *et al.* (2010) Experimental discovery of small RNAs in *Staphylococcus aureus* reveals a riboregulator of central metabolism. *Nucleic Acids Res.*, **38**, 6620–6636.
- Brantl, S. (2007) Regulatory mechanisms employed by cis-encoded antisense RNAs. *Curr. Op. Microbiol.*, **10**, 102–109.
- Morfeldt, E., Taylor, D., von Gabain, A. and Arvidson, S. (1995) Activation of alpha-toxin translation in *Staphylococcus aureus* by the trans-encoded antisense RNA, RNAlII. *EMBO J.*, **14**, 4569–4577.
- Boisset, S., Geissmann, T., Huntzinger, E., Fechter, P., Bendridi, N., Possedko, M., Chevalier, C., Helfer, A.C., Benito, Y., Jacquier, A. *et al.* (2007) *Staphylococcus aureus* RNAlII coordinately represses the synthesis of virulence factors and the transcription regulator Rot by an antisense mechanism. *Genes Dev.*, **21**, 1353–1366.
- Mangold, M., Siller, M., Roppenser, B., Vlamincs, B.J., Penfound, T.A., Klein, R., Novak, R., Novick, R.P. and Charpentier, E. (2004) Synthesis of group A streptococcal virulence factors is controlled by a regulatory RNA molecule. *Mol. Microbiol.*, **53**, 1515–1527.
- Wadler, C.S. and Vanderpool, C.K. (2007) A dual function for a bacterial small RNA: SgrS performs base-pairing dependent regulation and encodes a functional polypeptide. *Proc. Natl Acad. Sci. USA*, **104**, 20454–20459.
- Shimizu, T., Yaguchi, H., Ohtani, K., Banu, S. and Hayasi, H. (2002) Clostridial VirR/VirS regulon involves a regulatory RNA molecule for expression of toxins. *Mol. Microbiol.*, **43**, 257–265.
- Sonnleitner, E., Gonzalez, N., Sorger-Domenigg, T., Heeb, S., Richter, A.S., Backofen, R., Williams, P., Hüttenhofer, A., Haas, D. and Bläsi, U. (2011) The small RNA PhrS stimulates synthesis of the *Pseudomonas aeruginosa* quinolone signal. *Mol. Microbiol.*, **80**, 868–885.
- Roberts, S.A. and Scott, J.R. (2007) RivR and the small RNA RivX: the missing links between the CovR regulatory cascade and the Mga regulon. *Mol. Microbiol.*, **66**, 1506–1522.
- Berghoff, B., Glaeser, J., Sharma, C.M., Vogel, J. and Klug, G. (2009) Photooxidative stress-induced and abundant small RNAs in *Rhodobacter sphaeroides*. *Mol. Microbiol.*, **74**, 1497–1512.
- Licht, A., Preis, S. and Brantl, S. (2005) Implication of CcpN in the regulation of a novel untranslated RNA (SR1) in *B. subtilis*. *Mol. Microbiol.*, **58**, 189–206.
- Heidrich, N., Chinali, A., Gerth, U. and Brantl, S. (2006) The small untranslated RNA SR1 from the *B. subtilis* genome is involved in the regulation of arginine catabolism. *Mol. Microbiol.*, **62**, 520–536.
- Heidrich, N., Moll, I. and Brantl, S. (2007) *In vitro* analysis of the interaction between the small RNA SR1 and its primary target *ahrC* mRNA. *Nucleic Acids Res.*, **35**, 4331–4346.
- Licht, A., Golbik, R. and Brantl, S. (2008) Identification of ligands affecting the activity of the transcriptional repressor CcpN from *Bacillus subtilis*. *J. Mol. Biol.*, **380**, 17–30.
- Licht, A. and Brantl, S. (2009) The transcriptional repressor CcpN from *Bacillus subtilis* uses different repression mechanism at different promoters. *J. Biol. Chem.*, **284**, 30032–30038.
- Gimpel, M., Heidrich, N., Mäder, U., Krügel, H. and Brantl, S. (2010) A dual-function sRNA from *B. subtilis*: SR1 acts as a peptide encoding mRNA on the *gapA* operon. *Mol. Microbiol.*, **76**, 990–1009.
- Larkin, M.A., Blackshields, G., Brown, N.P., Chenna, R., McGettigan, P.A., McWilliam, H., Valentin, F., Wallace, I.M.,

- Wilm, A., Lopez, R. *et al.* (2007) Clustal W and clustal X version 2.0. *Bioinformatics*, **23**, 2947–2984.
24. Katoh, K., Misawa, K., Kuma, K. and Miyata, T. (2002) MAFFT: a novel method for rapid multiple sequence alignment based on fast Fourier transform. *Nucleic Acids Res.*, **30**, 3059–3066.
25. Posada, D. and Crandall, K.A. (1998) MODELTEST: testing the model of DNA substitution. *Bioinformatics*, **14**, 817–818.
26. Ronquist, F. and Huelsenbeck, J.P. (2003) MrBayes 3: Bayesian phylogenetic inference under mixed models. *Bioinformatics*, **19**, 1572–1574.
27. Eckart, R.A., Brantl, S. and Licht, A. (2009) Search for additional targets of the transcriptional regulator CcpN from *Bacillus subtilis*. *FEMS Microbiol. Lett.*, **299**, 223–231.
28. Kawamura, F. and Doi, R.H. (1984) Construction of a *Bacillus subtilis* double mutant deficient in extracellular alkaline and neutral proteases. *J. Bacteriol.*, **160**, 442–444.
29. Brantl, S. (1994) The *copR* gene product of plasmid pIP501 acts as a transcriptional repressor at the essential *repR* promoter. *Mol. Microbiol.*, **14**, 473–483.
30. Horler, R.S.P. and Vanderpool, C.K. (2009) Homologs of the small RNA SgrS are broadly distributed in enteric bacteria but have diverged in size and sequence. *Nucleic Acids Res.*, **37**, 5465–5476.
31. Stülke, J. and Hillen, W. (2000) Regulation of carbon catabolism in *Bacillus* species. *Annu. Rev. Microbiol.*, **54**, 849–880.
32. Servant, P., Le Coq, D. and Aymerich, S. (2005) CcpN (YqzB), a novel regulator for CcpA-independent catabolite repression of *Bacillus subtilis* gluconeogenic genes. *Mol. Microbiol.*, **55**, 1435–1451.
33. Wadler, C.S. and Vanderpool, C.K. (2009) Characterization of homologs of the small RNA SgrS reveals diversity in function. *Nucleic Acids Res.*, **37**, 5477–5485.
34. Göpel, Y., Lüttmann, D., Heroven, A.K., Reichenbach, G., Dersch, P. and Görke, B. (2011) Common and divergent features in transcriptional control of the homologous small RNAs GlmY and GlmZ in *Enterobacteriaceae*. *Nucleic Acids Res.*, **39**, 1294–1309.
35. Sharma, C., Darfeuille, F., Plantinga, T. and Vogel, J. (2007) A small RNA regulates multiple ABC transporter mRNAs by targeting C/A rich elements inside and upstream of ribosome-binding sites. *Genes Dev.*, **21**, 2804–2817.
36. Battistuzzi, F.U., Feijao, A. and Hedges, S.B. (2004) A genomic timescale of prokaryote evolution: insight into the origin of methanogenesis, phototrophy, and the colonization of land. *BMC Evol. Biol.*, **4**, 44.
37. Richard, A.L., Withey, J.H., Beyhan, S., Yildiz, F. and DiRita, V.J. (2010) The *Vibrio cholerae* virulence regulatory cascade controls glucose uptake through activation of TarA, a small regulatory RNA. *Mol. Microbiol.*, **78**, 1171–1181.
38. Papenfort, K., Podkaminski, D., Hinton, J.C. and Vogel, J. (2012) The ancestral SgrS RNA discriminates horizontally acquired *Salmonella* mRNAs through a single G-U wobble pair. *Proc. Natl Acad. Sci. USA*, **109**, E757–E764.